FORCE-FIELD DEVELOPMENT AND VALIDATION FOR STYRENE-ISOPRENE COPOLYMERS

A THESIS

submitted towards partial fulfillment of the requirements

for the award of

BS-MS Dual Degree Programme

by

AISHWARY SHIVGAN

(20111069)

Under the guidance of

DR. INDRANIL RUDRA

Shell Technology Center, Bangalore

DEPARTMENT OF CHEMISTRY
INDIAN INSTITUTE OF SCIENCE EDUCATION AND RESEARCH PUNE
PUNE - 411008

CERTIFICATE

This is to certify that this dissertation entitled **"Force-field development and validation for Styrene-Isoprene copolymers"** towards the partial fulfilment of the BS-MS dual degree programme at the Indian Institute of Science Education and Research, Pune represents the research carried out by **"Aishwary Shivgan"** at "**Shell Technology Center, Bangalore (STCB)**" under the supervision of **"Dr. Indranil Rudra, Research Scientist, Center for computational Expertise (CcoE)"** during the academic year 2015-2016.

Indranil Rudra

Dr. Indranil Rudra
Thesis Supervisor

DECLARATION

I hereby declare that the matter embodied in the report entitled **"Force-field development and validation for Styrene-Isoprene copolymers"** are the results of the investigations carried out by me at Shell Technology Center, Bangalore under the supervision of Dr. Indranil Rudra, Center for computational Expertise (CcoE) and the same has not been submitted elsewhere for any other degree.

Aishwary Shivgan
(20111069)

ACKNOWLEDGEMENT

I thank my supervisor Dr. Indranil Rudra, Center for Computational expertise, Shell. His expertise and in-depth understanding of the field constantly proved to be a great guidance for me in conducting my research. I am indebted to him for having the confidence in me for such an endeavor.

I am grateful for getting the opportunity to work with Dr. Sudip Roy, Shell Technology center, Bangalore who made immense efforts to help me understand the computational aspects of polymer physics. I am thankful to him for training me in conducting research at such a level.

My sincere thanks goes to Dr. Vetrivel Rajappan, and Dr. Vianney Koelman, for offering me the internship opportunity in their group and leading me working on this exciting project.

I thank Dr. Srabanti Chaudhuri, Assistant Professor, IISER Pune who kept me motivated towards my Master's thesis project with her constant feedback and played an important part in making this possible.

I thank Shell Technology Center, Bangalore which played an important role in providing computational resources. I thank IISER Pune and everyone who supported me to make this research experience a success.

Aishwary Shivgan

CONTENTS

LIST OF FIGURES

LIST OF TABLES

ABSTRACT

Copolymers are interesting kind of macromolecules and have found many applications. Styrene-Isoprene copolymers are used as additives in the fuels to improve their Viscosity Index (VI). A fuel with a good VI is the one which has low viscosity-temperature dependence.

I this masters thesis, we have developed a all-atomistic forcefield for these copolymers. The dihedrals and partial charges were calculated using quantum chemical calculations. MD simulations of the Styrene-Isoprene and Styrene-Isoprene (Hydrogenated) copolymers with different compositions. The MD simulation data have been analyzed to provide information about density dependence on the copolymer chain length in order to find minimum chain length that needs to be used in order to get a polymeric behaviour. The simulated annealing technique was used for calculating the glass transition temperatures of different compositions of copolymers. It was found that both the copolymers have linear density dependence on the copolymer compositions. Glass transition temperature follows a similar trend for both the copolymers.

N-decylbenzene and n-hexadecane were used as a base oil (diesel surrogates) to study the viscosity modification property of these copolymers. Our calculations using Green-Kubo method shows that the copolymers indeed enhance the viscosity of the base oil. Comparing the block and tapered copolymers, we observed that block copolymer increases the viscosity comparatively higher than the corresponding tapered copolymer. Tapered copolymer works better as Viscosity Index Modifier (VIM), as the viscosity-temperature dependence is lower compared to the block copolymers. The radius of gyration was observed to be smaller for tapered than block copolymer which results in a lower interaction of the tapered copolymer with the base oil, hence lower viscosity enhancement compared to a block copolymer.

LIST OF SYMBOLS OR ABBREVIATIONS

$\hat{H}$	Hamiltonian
ψ	Wave-function
k_B	Boltzmann constant
ϵ	Dielectric constant
A	Helmholtz free energy
ρ	Density
η	Viscosity

1. INTRODUCTION

Understanding of polymers has been of importance from different perspectives. They have applications in industry, biological relations, medicines and so on. In this chapter, we discuss the polymer's important property of modifying the viscosity of a fluid.

1.1 Polymers as Viscosity Index Modifiers

Rheological properties of hydrocarbons are special interest in the petroleum and automobile industry. Predicting these properties using computer simulations as well as theoretical approach has intrigued ample interest in the scientific community.[2] One such important property is the shear Viscosity. Refined petroleum oils generally suffer from changes in viscosity with temperature. An oil should be able to flow at low temperatures to assist in cold starting of the engine. Also at high temperatures it should not become so thin that it is not able to maintain it's load-bearing properties.[3] An ideal fuel should not have a large change in viscosity with the change in the temperature. Viscosity Index[4] (VI) measures the change in viscosity with temperature. Higher the VI lower the viscosity-temperature dependence. There are different additives that are added in the base oil to improve its efficiency as well as resistance to different conditions. One such additive which improves the viscosity index is called as Viscosity Index Modifiers (VIM's).

Most common VIM's are polymeric molecules[5,6] which are sensitive to temperature. Polymers are large molecules comprising of repeated subunits. They have a wide range of properties. They can be synthetic such as polystyrene, synthetic rubber, neoprene, nylon, polyethylene or natural polymers such as DNA, wool, natural rubber, cellulose.

Polymer containing fluids show less reduction in viscosity when compared to the viscosity of the fluid with no polymer. When we add large molecules (polymers) in small molecules (fuel), the large molecules restrain the motion of small molecules which can be manifested to the increase in the viscosity. They have a specific hydrodynamic volume which increases upon the increase in the temperature, hence compensating the general effect of reduction in the viscosity of fuels with temperature. A compatible solvent is needed to for the Viscosity index improvement as solvent interacts the polymer links resulting in swelling effect needed for VI improvement. Opposite effect would be observed in the presence of poor solvent[1] as shown in fig. (1.1).

The experimental prediction of the viscosity has been pursued but theoretical prediction of this property will result in understanding of this process at a molecular level. This will help experimentalist in not having to prepare those samples which increase the cost as well as the hazards involved in preparing those. These models will enable

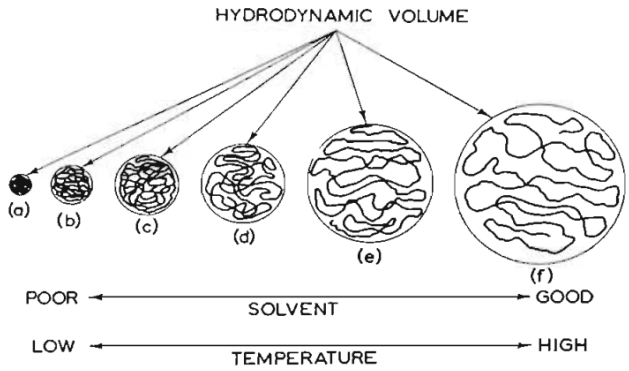

Fig. 1.1: Expansion and contraction of a macromolecule[1]

us to study the properties at extreme conditions otherwise which were not possible in experimental conditions. We could tweak the topology and composition according to our liking and test whether the model is better VIM compared to already available ones. So it is desirable to have a computational model for these widely used viscosity index modifying polymers and this is the motivation for the project.

Molecular dynamics has emerged to be a powerful technique to study static as well as dynamic properties of different systems including polymers.[2,7] In this thesis, we have worked on the molecular dynamics (MD) simulations of copolymers composed of Styrene, Cis-1,4 Isoprene and hydrogenated Isoprene (fig. 1.2), the properties of which described in further sections.

1.2 Polystyrene

Polystyrene is a common commercial polymer and it is most widely studied among all amorphous polymers. Polystyrene is generally rigid but can be foamed called as Styrofoams which are used as thermo-insulators. Polystyrene is hard in nature and also brittle. The inexpensive nature has made it one of the most industrially important polymer.[8,9]

1.3 Poly-Isoprene

Cis-1,4 Polyisoprene (PI) is the main constituent of the Natural rubber which can be also synthesized using petroleum byproducts. The physical properties of the polymer as the name suggests are unique. The polymer has toughness as well as extensibility. The polymer can be stretched repeatedly several times. The polymers remain in the amorphous state without the presence of stress. On being applied the stretching force the molecules gets aligned in a crystalline arrangement which leads to greater strength hence also know as ”self-reinforcing”. Due to the presence of the double bond, PI reacts with oxygen and ozone present in the atmosphere. This leads to degradation of the polymer mainly rupturing and softening.[10]

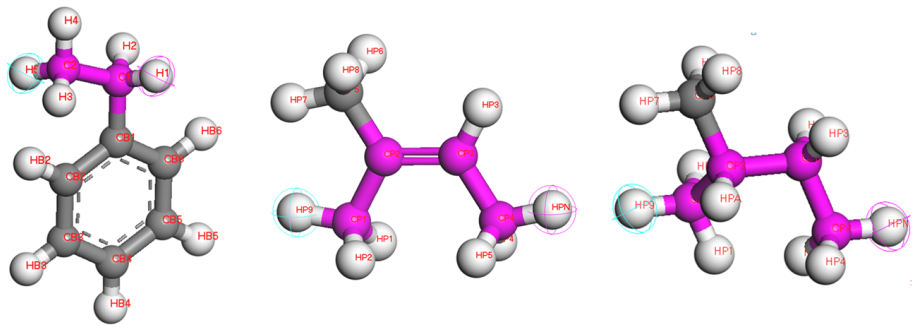

Fig. 1.2: (a) Styrene (b) Cis-1,4-Isoprene and (c) Isoprene Hydrogented

1.4 Poly-Isoprene (Hydrogenated)

Polymers made from cis-1,4 isoprene suffers from chemical degradation mainly oxidation. This happens due to reactive double bond in the isoprene. One of many chemical modification techniques to circumvent this problem is to hydrogenate it and is been practiced regularly.[11] The Hydrogenated polyisoprene (IsoH) has similar properties of Polyisoprene. Chemical modification of polymers such as hydrogenation is used to reduce the saturation which enhances the thermal resistance of the polymers. Also it gives the oxidative resistance leading to increase in the life span of the polymers.[12] Hydrogenation removes the double bonds in the molecule which reacts with oxygen and ozone. Hence greatly improving the thermo-oxidative stability.

1.5 Copolymers

Copolymers are a fascinating class of polymer materials and has interested many scientists and engineers. They are composed of covalently joined two or more non miscible blocks and combines the properties of individual homopolymers. Polystyrene is rigid and has a high glass transition temperature (T_g) while polyisoprene is called as synthetic rubber for its highly elastic behavior and has a low T_g. Combining the two in the form of copolymers gives rise to new properties, controlled by the composition of components and their molecular weight.[13] These copolymers mainly Styrene-isoprene and styrene-isoprene (hydrogenated) have been studied greatly in scientific community due to their practical uses[11,14] importantly their use as viscosity index modifier (VIM).

The objectives of the studies are as follows:

- Making a framework for building copolymers of Sty, Iso and IsoH with different topologies including diblock, random block and tapered.
- Use homopolymer all atomistic models from the literature and use them for copolymers. Calculate the parameters exclusive to the copolymers of Sty, Iso and IsoH.
- Predict the densities as well as glass transition temperatures of copolymers with different compositions.

- Use n-hexadecane (hex) and n-decylbenzene (dec) as a base oil. Validate various all-atomistic models and use the best one for the viscosity calculations.
- Predict the viscosity of the solvent (n-hexadecane + n-decylbenzene) and copolymer mixture as a function of composition of the solvent with different temperature and pressure conditions.
- Compare between viscosity modifying properties of the different topologies of copolymers such as block and tapered copolymer.

2. THEORY

This section describes the computational methods used for the study of Styrene (Sty), Isoprene (Iso) and Isoprene-hydrogenated (IsoH) copolymers. We have used quantum calculations and molecular dynamics simulations for this study. Green-Kubo method was used for the viscosity calculations.

2.1 Quantum chemical calculations

Ab-initio calculations does not depend on any empirical information such as parameters, potentials and only depends on established laws of nature being quantum mechanics in which one tries to solve Schrödinger equation.

$$\hat{H}\psi = E\psi \tag{2.1}$$

Where ψ is the wavefunction, H is the Hamiltonian and E is the energy of the system. But only a limited number of systems such as the rigid rotor, harmonic oscillator, particle in a box and hydrogenic ions have exact solutions. Hence, approximations such as Hartree-Fock theory where wave-functions are used for the calculations, Density Functional Theory where the electron density is used instead of complicated wave-function are being used. In our studies, we have used DFT calculations which uses a wave approach.

$$\psi_i(\mathbf{r}) = \exp(i\mathbf{k}.\mathbf{r})f_i(\mathbf{r}) \tag{2.2}$$

Where $f_i(\mathbf{r})$ can be expressed in terms basis set. A basis set is a set of non-orthonormal one-particle functions (basis functions) which are combined in linear form to create a molecular orbital. With recent advancements in computational resources as well as efficient algorithms now we can now predict structures, energies, reactivities and many other properties of molecules at great accuracy. Still, the method is limited to few hundred atoms.[15] Hence, the parameters such as bonds, angles, dihedral potentials, partial charges are calculated using this method for a small system and used as input in the molecular dynamics algorithm which enables us to reach higher lengthscales and timescales. GAUSSIAN program was developed by John Pople.[16] We have used the version 03 for our calculations in this thesis project.

2.2 Molecular dynamics(MD)

Many of the real-life problems that we would like solve, unfortunately, involve big molecules like polymers which are too large to be worked with quantum mechanics. Even if some of the electrons are ignored like in the semi-empirical methods, still the calculations will be very time-consuming and the system size will be limited temporally as well as spatially. Forcefield methods also known as molecular dynamics (MD), ignore

the electronic motions. These methods calculate the energy of the system based only on nuclear positions. This enables us to go higher timescales (μs) as well as length-scales (nm). In some cases, forcefield provides the energies as accurate as quantum mechanics within a fraction of the time.

Most widely used simulations techniques for studying such large systems are Molecular Dynamics (MD) and Monte Carlo (MC). In Monte Carlo methods relies on random sampling to calculate the probability of different outcomes. MD uses classical newton's equation of motions to determine the time evolution of positions and velocities.[15] Generally, MD methods are preferred over MC methods because these simulations give essential information about atomistic motions of molecules with time. Theses MD simulations are dependent on forcefield potential parameters which can be tweaked according to the property being targeted.

2.2.1 Basic concepts

Before jumping to Molecular Dynamics some basic concepts of statistical mechanics are useful. If we take a particle in a box, then the motion of that particle can be described using three spatial and three momentum coordinates. This creates a six-dimensional phase space in which each point defines a state of the system. Now if we take N number of particles in a box we will have the 3N position as well as 3N momentum coordinates. This creates 6N dimensional phase space. The system can be denoted by $(\mathbf{p},\mathbf{q})$, where **p** and **q** are generalized positions and momentum for N particles.

As the system evolves over time through the phase space, the dynamics of the motion can be described using Hamiltonian $H(\mathbf{p},\mathbf{q})$. The motions can be given by following equations:

$$\frac{d\mathbf{q}_i}{dt} = \frac{\partial H(\mathbf{p},\mathbf{q})}{\partial \mathbf{p}_i} \quad \text{and} \quad \frac{d\mathbf{p}_i}{dt} = \frac{\partial H(\mathbf{p},\mathbf{q})}{\partial \mathbf{q}_i} \qquad \text{where} \quad i = 1,\ldots,N \tag{2.3}$$

The particle can only span phase space which is accessible to it by applying statistical ensemble. For e.g under constant number, volume, energy (NVE) ensemble the particle can go to the point in phase space which satisfies the condition $H(\mathbf{p},\mathbf{q}) = E$. The particle can now roam around constant energy surface. Under the constant NVT ensemble, the system energy is allowed to fluctuate but the temperature is fixed where the probability of each phase point is proportional to

$$E \propto \exp\left(\frac{-A}{k_B T}\right) \tag{2.4}$$

Where k_B is the Boltzmann constant, T is the temperature, A is the Helmholtz free energy of the system. For the isothermal-isobaric (NPT) ensemble the probability of state is proportional to following term and in the thermodynamic limit all ensembles produce the same results.[15]

$$E \propto \exp\left(\frac{-PV}{k_B T}\right) \tag{2.5}$$

Once we define the ensemble under which the simulation should be performed the velocities and positions are updated using leap-frog algorithm. Positions at time t and velocities at time $t - t/2$ are used to calculate the next positions and velocities using forces $F_i(t)$ acting on atom i at time t.

$$x(t + dt) = x(t) + \frac{dx(t)}{dt}(t + dt/2)dt \tag{2.6a}$$

$$\frac{dx(t)}{dt}(t + dt/2) = \frac{dx(t)}{dt}(t - dt/2) + \frac{d^2x(t)}{dt}dt \tag{2.6b}$$

MD simulations scale as a $O(N^2)$ where N is the number of atoms in the simulation.

Global Molecular Dynamics algorithm

1. Input conditions

Potentials for the interaction between atoms
Velocities and positions of the all atoms in the system

⇓

Repeat following procedure for the required number of steps

2. Calculate forces

The force on i^{th} atom

$$\mathbf{F}_i = -\frac{\partial V}{\partial \mathbf{r}_i}$$

is calculated using the forces on i^{th} atom due to non-bonded and bonded pairs, plus any external or restraining forces

$$\mathbf{F}_i = \sum_j F_{ij}$$

Potential and kinetic energies are calculated

⇓

3. Updating the configuration

Numerically solve the Newton's equations to move the atoms to next position in time t

$$\frac{d^2\mathbf{r}_i}{dt^2} = \frac{\mathbf{F}_i}{m_i}$$

⇓

4. Corrections

Apply boundary conditions, temperature and pressure control as needed

⇓

5. Output

Write properties of interest to get evolution of the system as a function of time

This becomes computationally expensive for simulating large systems using MD. A general molecular dynamics algorithm is as above. The forces needed for the calculation are obtained from forcefield provided for the MD simulations.

2.2.2 Force-field

A potential energy landscape V(**R**) or forcefield is required by the MD simulations to describe atomic interactions during each step of the simulation. Forcefield gives the mathematical form of potential energy that is used to describe the different types of interactions between the atoms in the MD simulations. A forcefield has bonded and non-bonded interaction terms given by following equations.

$$V_{total} = V_{bonded} + V_{non-bonded} \tag{2.7}$$

$$V_{total} = V_{bonds} + V_{angles} + V_{dihedrals} + V_{electrostatic} + V_{van-der-Waals} \tag{2.8}$$

In our work, we have primarily worked with Optimized Parameters for Liquid Simulations[17] (OPLS) all atom force-field. The potential forms used for different bonded and non-bonded terms used by this forcefield are given below. Bonds are defined by the simple harmonic equation given by

$$V_b = \frac{1}{2} k_r (r_{eq} - r)^2 \tag{2.9}$$

Where r_{eq} is the equilibrium bond length and r is the distance between bonded atoms. The angles are also defined using simple harmonic form

$$V_\theta = \frac{1}{2} k_\theta (\theta_{eq} - \theta)^2 \tag{2.10}$$

Where θ_{eq} is equilibrium angle while θ is the angle between the two bonds. The dihedrals are important for achieving a specific conformation and are defined using the following function

$$V_d = k_\phi (1 + \cos(n\phi - \phi_s)) \tag{2.11}$$

Where n is the multiplicity, ϕ is the dihedral angle between two planes obtained by atoms i, j, k and j, k, l and ϕ_s is the phase shift. The non-bonded interactions includes electrostatic as well as the Van-Der-Waals interactions. The total non-bonded interactions are given by

$$V_{nb} = \sum_i \sum_j (elctrostatic_{ij} + Lennard - Jones_{ij}) f_{ij} \tag{2.12}$$

Where f_{ij} is a fudge factor and is equal to 1.0 except for intermolecular 1,4-interactions where f_{ij}=0.5. The Lennard-Jones potential is a simple pair potential described by

$$V_{LJ}(r_{ij}) = 4\epsilon_{ij} \left(\left(\frac{\sigma_{ij}}{r_{ij}} \right)^{12} - \left(\frac{\sigma_{ij}}{r_{ij}} \right)^{6} \right) \tag{2.13}$$

Where σ is the the finite distance at which the inter particle potential is zero, ϵ is the depth of the potential well and r is the distance between i^{th} and j^{th} atoms. The mixing rules for σ_{ij} and ϵ_{ij} are given by

$$\sigma_{ij} = (\sigma_{ii}\sigma_{jj})^{1/2} \quad \text{and} \quad \epsilon_{ij} = (\epsilon_{ii}\epsilon_{jj})^{1/2} \tag{2.14}$$

Electrostatic interactions were calculated using Reaction field[18] (RF) method. The potential which is given by

$$V(\mathrm{erf}) = f\frac{q_i q_j}{\epsilon_r}\left[\frac{1}{r_{ij}} + k_{rf} r_{ij}^2 - c_{rf}\right] \tag{2.15}$$

Where q_i and q_j are the partial charges on the interacting atoms. k_{rf} is related to the dielectric constant ϵ_{rf} and c_{rf} is related to cut-off r_c.

2.3 Green-Kubo Viscosity calculation

There are many equilibrium as well as non-equilibrium methods for determination of the viscosities of the fluid from MD simulations.[19] The equilibrium methods use pressure or momentum fluctuations[20] to calculate the viscosity. In our simulations, we have used Green-Kubo equilibrium method for the calculations of the viscosities of the fluid containing copolymers and solvent. Green and Kubo[21,22] showed that the shear viscosity could be determined from the fluctuations in the pressure tensor of a system in a thermal equilibrium. Viscosity is calculated by integrating the Green-Kubo formula.[23]

$$\eta = \frac{V}{k_B T}\int_0^\infty \langle P_{xz}(t_0) P_{xz}(t_0 + t)\rangle_{t_0} dt \tag{2.16}$$

Where k_B is Boltzmann constant. P, V and T are the pressure, volume and temperature of the system respectively. In principle, to use this equation for calculating viscosity, t should be sufficiently large. But this is not possible to computational limitations. Hence finite time period t' is used for the calculations.

$$\eta(t') = \frac{V}{k_B T}\int_0^{t'} \langle P_{xz}(t_0) P_{xz}(t_0 + t)\rangle_{t_0} dt \tag{2.17}$$

3. METHODOLOGY

In this chapter we discuss about the framework used for generating different copolymers including tapered and block, optimization of dihedral parameters and partial charges using GAUSSIAN03. All-atomistic MD simulations have been used to validate the forcefield with experimental data using density, glass transition temperature (T_g) and viscosity of the copolymers.

3.1 Universal topology

The study focuses on making atomistic co-polymer forcefield having Sty, Iso and IsoH as constituents of the copolymer. This gives many possible combinations in which we can form connections between Sty, Iso and IsoH. The different connections such as Sty-Sty-Sty-Iso-Iso-Iso, Sty-Sty-Iso-Iso-Sty-Sty, Sty-Iso-Sty-Iso are required for describing the different topologies. Taking into account that the reaction goes through cationic or radical mechanism, it reduces the different unique connections to 16. The sixteen different types of residues used in defining the topology are shown in Fig. 3.1.

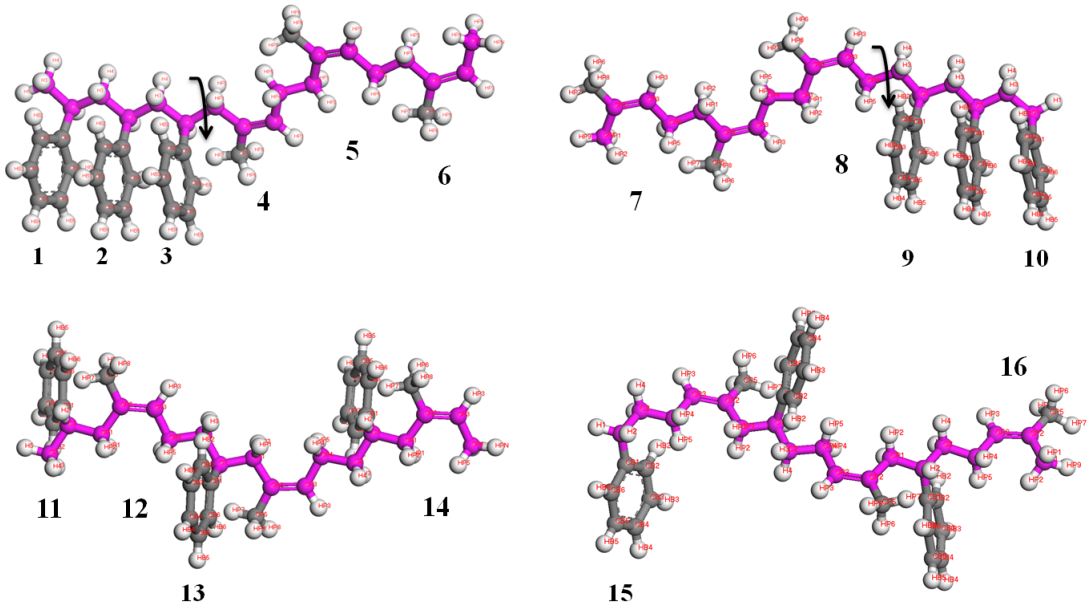

Fig. 3.1: Different residue types defined in residue topology file

To start with the models for Sty, Iso and IsoH monomers were created using Material Studio 7. The copolymers were created using the 'build copolymer' function in the same.

3.2 Forcefields

Natural rubber consists of both the cis and trans form but the cis-1,4-polyisoprene is the major constituent. Both the forms of the 1,4-Polyisoprene have been widely studied in the scientific community. Different studies such as self-diffusion properties, the temperature dependence of densities, diffusion coefficients[2] have been done. Many computational models have been developed for Poly-isoprene[24,25] has been used in many studies.[26,27] The forcefield developed by Sudip *et. al*[25] was used for Cis-1,4-polyisoprene which is good at producing densities and glass transition temperatures in good agreement with experimental values.

Various computational models[28,29] exists for polystyrene, which are good at reproducing the densities at different pressure and temperature conditions. Modeling of this polymer at the atomistic level, using either MD[7,30] or MC[31] methods has been widely practiced. These studies worked on the dynamical as well as structural properties of bulk polystyrene. The all-atom model developed by Qian *et.al.*[32] is used in our studies, which is a OPLS-AA based force field.

Hydrogenated isoprene is not a widely studied polymer with very few experimental studies and no computational studies. So, to start with IsoH polymer was modeled using the OPLS-AA[17] parameters without any modification.

3.3 Dihedral Calculation

The individual forcefields for the homopolymer have all the bonded and nonbonded terms except the dihedral potential and partial charges for Sty-Iso and Sty-IsoH connections. The dihedrals were calculated using software Gaussian03. The initial structure was geometry optimised using B3LYP hybrid-functional with 6-31g(d,p) basis set. A potential energy scan was performed on the geometry optimised structure, in which a particular dihedral is selected then the structure is optimized and energy is calculated. Then selected dihedral angle is increased by fixed angle then optimized again giving the energy of structure with the new dihedral angle. The process is continued till the dihedral angle is scanned by 360 degrees. The calculations were done using B3LYP hybrid-functional with 6-31g(d,p) basis set. The results are shown in fig. 3.3 and were fitted to the function 3.1.

$$V_d(\phi_{ijkl}) = \sum_n k_\phi(1 + \cos(n\phi - \phi_s)) \tag{3.1}$$

Where i, j, k and l are the four atoms connected, n is the multiplicity and ϕ_s is the angle which is obtained from fit. In our simulation, dihedral scan with step size of 20° was performed.

3.4 Partial charge calculation

The partial charges for connecting residues showed in fig.(3.2) were calculated using CHarges from ELectrostatic Potentials using a Grid-based (CHELPG)[33] method. In

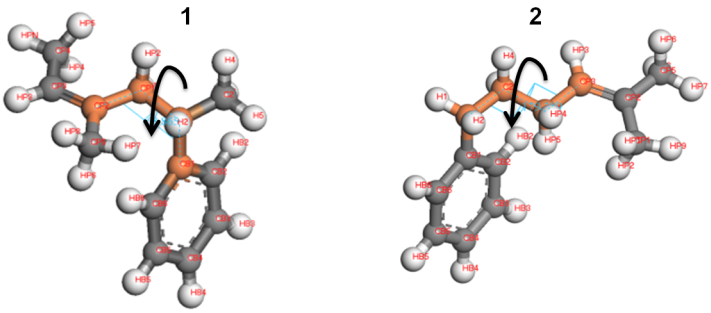

Fig. 3.2: Dihedral required for Sty-Iso connections

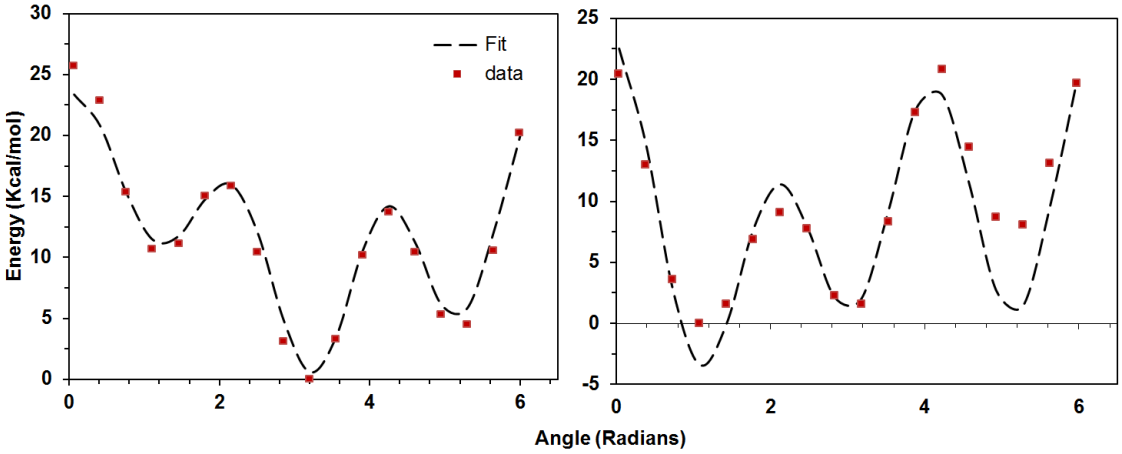

Fig. 3.3: Dihedral scan data for dihedrals 1 (left) and 2 (right) with fit to eq.(3.1)

this method, one tries to reproduce electrostatic potentials by fitting atomic charges (MESP). 6-311g(d,p) basis set was used with B3LYP hybrid functional.

3.5 GROMACS parameters

The calculated dihedral parameters and partial charges were used to define different residues in fig. (3.1) in residue topology file (.rtp) of GROMACS 4.6.7[34] molecular dynamics simulations package. Intramolecular nonbonded interactions were calculated for the atoms separated by at least two or three bonds. The LJ and Coulomb interactions (1,4) were scaled down by a fudge factor of 0.5. Motions of the molecules were handled using Leap-from integrator. The energy minimizations with a tolerance of 10 KJ/mol/nm were performed using steepest descent algorithm.

3.5.1 NPT and NVT equilibration

The isothermal-isobaric equilibration was done using Berendsen thermostat[35] with a coupling constant of 0.5 ps. The Berendsen barostat[35] with coupling constant of 0.5 ps and compressibility of $4.5e^{-5}$ was used in our simulations. All bonds were constrained using LINCS[36] algorithm which allows us to use higher timestep (2 femtoseconds) by constraining high-frequency motions such as bonds. The electrostatic inter-

actions were calculated using RF method[18] beyond the cut off of 1.2nm and dielectric constant of 4.

Canonical ensemble (NVT) production runs were performed for the viscosity calculations using same parameters as NPT ensemble but without the Berendsen barostat. No constraints were applied and the timestep of 0.5 femtoseconds was used.

3.6 Co-polymer chain length

In reality, the polymers are composed of thousands of monomers. Due to computational limitations, such high chain length and number of polymers can't be used in the simulations. Instead, a particular chain length is used such that a particular property converges and produces a value similar to the experimental value. The study was done by using monodisperse polymers. A single copolymer chain was energy minimized using steepest descent algorithm then NPT simulation at pressure 1 bar and temperature 298K was performed on the same single chain. A simulation box was constructed by randomly inserting polymer chains with final configuration from previous NPT run. The box packed with polymer chains was again energy minimized. NPT simulation at temperature 298K and pressure 1bar was performed until the density equilibrated. The density was calculated from equilibrated simulation box. Same calculation was repeated with different chain lengths of the copolymer.

The dependence of the density on chain length was studied. The chain length after which the change in density is minimal was used for further calculations. This chain length will be a minimum chain length one should use for getting a polymeric behavior.

3.7 Glass transition temperature

Polymers are characterized by their unique glass transition temperature or T_g. The glass–liquid transition is a reversible transition from a hard or solid like state to molten or rubber-like state and it is reversible. A copolymer has the glass transition temperature in the range of constituent homopolymer's T_g's. In this case, polystyrene has a T_g of 373 °C,[37] polyisoprene has a T_g of 200 °C[38] and polyisoprene hydrogenated has a T_g of 213 °C.[39] Depending upon the compositions, copolymers will show a T_g between 200 ° and 373 °C for Sty-Iso copolymers and between 213 ° and 373 °C for Sty-IsoH copolymers.

Glass transition temperature is highly configuration dependent, so the structure needs to be highly energy minimized with configuration same or similar to the global minimum. Simulated annealing is a fast method to achieve a global or approximate global minimum, during which temperature of the system is raised so that even if the system is stuck in a local minimum, the system gets enough energy to cross the potential energy barrier. In our simulations, simulated annealing cycle consists of temperature steps of 50 °. The heating cycle started from 150 °, 200 ° to 600 °, 650 °C and the reverse for cooling. At each temperature, the system was equilibrated for 3ns then the temperature was ramped up to next temperature within 1ns and the process was

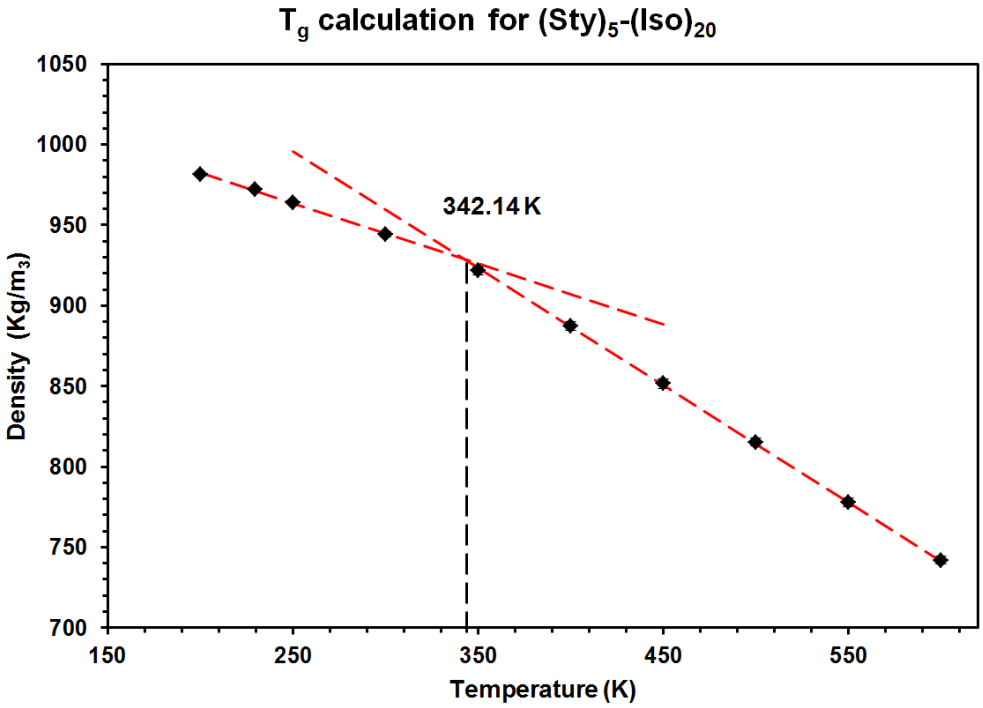

Fig. 3.4: Density vs Temperature for $(Sty)_5 - (Iso)_{20}$

continued. This gives us a heating and cooling rate of 11.36 K/ns. Simulation annealing cycles (heating and cooling) were performed on all copolymer compositions until the potential energy of the systems decayed to a constant value. This ensures that the final system is in a reasonable low-energy state. The final cycle was used for extraction of the coordinates at different temperatures and they were equilibrated using constant temperature and pressure for 10 ns. This gives us the rate of 4.13 K/ns. We believe this rate is slow enough to get the approximate value of T_g for the final cycle. The Density vs temperature was plotted.

An example of a T_g calculation for the copolymer $(Sty)_5 - (Iso)_{20}$ is shown in the figure 3.4. It is observed from the plot that slope of density vs temperature above and below the T_g is different. The Same effect is observed by dilatometry, DSC and dynamic mechanical analysis experiments.[9] The plot was fitted above and below T_g with a straight line to get T_g as the intersection point of the two fitted lines. The similar protocol was repeated for different compositions.

The T_g's calculated for different compositions were fitted with empirical equation given by Kwei[40] for diblock copolymers given that homopolymer's T_g's are known.

$$T_g = \frac{x_1 T_{g1} + k_{kw}(1 - x_1) T_{g2}}{x_1 + k_{kw}(1 - x_1)} + q x_1 (1 - x_1) \tag{3.2}$$

Here x_1 and T_{g1} are the mole fraction and glass transition temperature of the homopolymer having low T_g of the two homopolymers and x_2, T_{g2} are the mole fraction and T_g for homopolymer with higher T_g. k_{kw} and q are the Kwei's parameters obtained from the fit.

3.8 Viscosity calculations

Green-Kubo method as described in the section 2.3 was used for viscosity calculations. Timestep of 1 fs for the UA model and 0.5 fs was used for the AA model. The final box volume from the NPT run was used to carry out a constant NVT simulation for a period of 2 ns. The final coordinates of this NVT run were used for the initial configuration for ten different constant NVT runs. These short simulated annealing runs were carried out at different temperatures such as 425, 430, 435, 440, 445, 450, 455, 460, 465 (all in Kelvin) for calculating viscosity at 423k. The run length at each of these temperatures was 1 ns. The systems were then quenched back to 423K over a duration of 1ns. The process was done in order to get different independent trajectories. At 423K, a constant NVT MD trajectory was generated for 3ns in each of these independent runs. A similar approach was used for calculating viscosity at different temperatures. The distinct elements of the stress tensor were stored every time step. The stress-stress time correlation function was calculated using a Green-Kubo analysis code.

The purpose of using ten independent trajectories is to allow us to sample a larger phase space. This is very important to simulate a collective property like viscosity. In addition, there is a possibility that in a single trajectory the system may get trapped in a local minimum configuration which will lead to possibly an erroneous value for viscosity. This possibility can be mitigated by running multiple independent trajectories and averaging over their individual viscosities. The number of trajectories that needs to be considered would depend upon the number of degrees of freedom the system has. Also, one can carry out simulations of long enough time length and the same viscosity value could be obtained from that single trajectory which has reached its true equilibrium.

4. RESULTS AND DISCUSSION

The two copolymers studied are Sty-Iso and Sty-IsoH. We have started with density calculation as a function of composition. later, we have calculated the gas transition temperature for each copolymer composition.

4.1 Styrene-Isoprene Copolymer

4.1.1 Densities

The homopolymers of styrenes and Isoprenes were constructed and the density as a function of chain length was calculated as described in the section 3.6. It can be seen from the plot 4.1 that the plot plateau's at $(\mathrm{Sty})_{10}$ with the density of 1052.5 $\mathrm{kg/m^3}$ with an error of 0.24% from the experimental value of 1050 $\mathrm{kg/m^3}$ at 298K. A similar calculation was done for polyisoprene which plateau's for $(\mathrm{Iso})_{40}$. Iso_{40} produces a density of 905.32 $\mathrm{kg/m^3}$ with deviation of 0.51% from the experimental value of 910 $\mathrm{kg/m^3}$. We believe the chain length of 10 and 40 is enough for showing a polymeric behavior for polystyrene and polyisoprene respectively. This exercise was done in order to select the appropriate chain length for the density, T_g and viscosity calculations. As these chain lengths give the densities in a good agreement with experimental values, they were used for glass transition temperature calculations.

Homopolymer forcefields gave good densities compared to experimental data hence were used for Sty-Iso copolymers with different compositions. After calculating the dihedral potentials and partial charges as described in the sections 3.3 and 3.4 different compositions of copolymers were created using Material Studio 7. Again the for each compositions, such lets say if a copolymer has a 24.64% Iso content by weight then different chains such as $(\mathrm{Sty})_6-(\mathrm{Iso})_3, (\mathrm{Sty})_8-(\mathrm{Iso})_4, (\mathrm{Sty})_{10}-(\mathrm{Iso})_5, (\mathrm{Sty})_{20}-(\mathrm{Iso})_{10}$ and $(\mathrm{Sty})_{30}-(\mathrm{Iso})_{15}$ could be constructed wherein all the chains have the percentage of the Iso. Simulations systems were created each with a particular chain length and densities were obtained after NPT equilibration.

It can be seen from the plot 4.1 that every composition of co-polymers (Sty-Iso) has a chain length dependence. The fig: 4.2(a) shows the minimum chain length required for the polymeric behavior and the density obtained with that chain length. Fig. 4.2(b) shows density density dependence on the composition, the plot follows a linear trend, which is a characteristic of many block copolymers.

4.1.2 Glass transition temperatures (T_g) :

The chain lengths obtained from the previous calculations were used for the calculations of the T_g for homopolymers and copolymers. The similar protocol as described

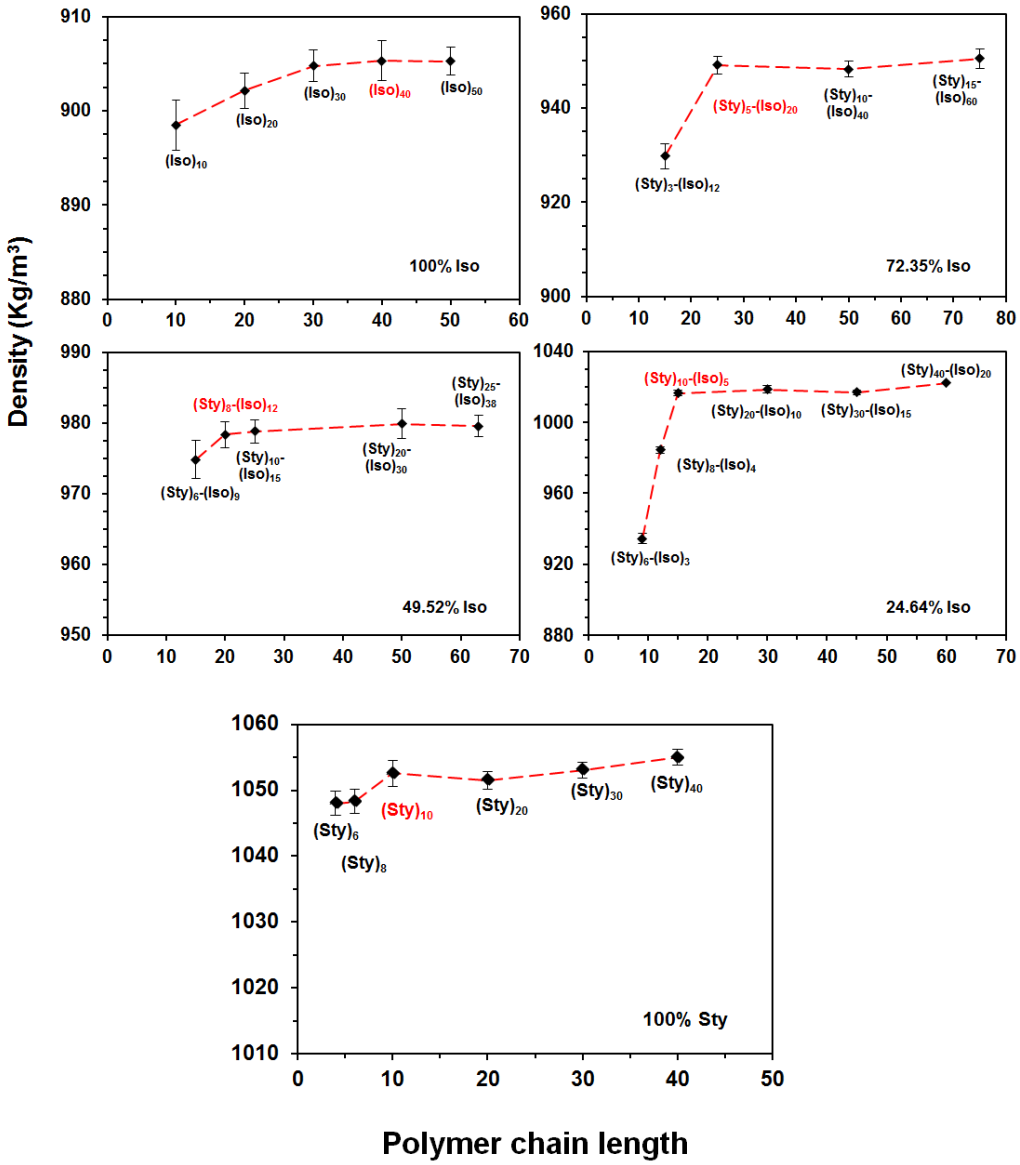

Fig. 4.1: Dependence of density on the chain length for different compositions of the Sty-Iso copolymer

in the section 3.7 was used for the T_g calculation for every composition starting with simulated annealing cycles followed by NPT run (10ns) at each temperature. The dependence of T_g on the composition is plotted in the figure 4.3.

The simulations data follows the similar trend as experimental data.[9,13] $(Sty)_{10}$ gives a T_g of 401 K with a error of 7.71% from the experimental value of 373 K while $(Iso)_{40}$ gives a T_g of 233 K with a error of 16.59% from the experimental value of 200K. The T_g vs compositions follows the similar behavior as many copolymers.[41] The T_g values are overestimated for the different compositions of copolymers from the experimental data[13] which could be attributed to fast heating and cooling rates of 4.13 K/ns used in the simulation and has also known to affect the T_g's in experimental conditions.[42]

The Sty-Iso forcefield results (density and glass transition temperature) are described in the table 4.1.

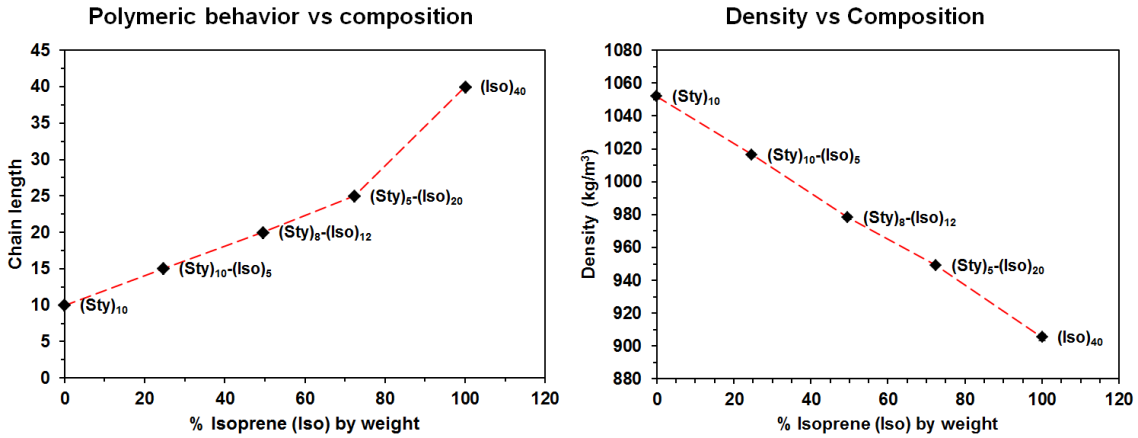

Fig. 4.2: Left: (a) Minimum chain length required for the polymeric behaviour right: (b) Density as a function of composition for Sty-Iso copolymers

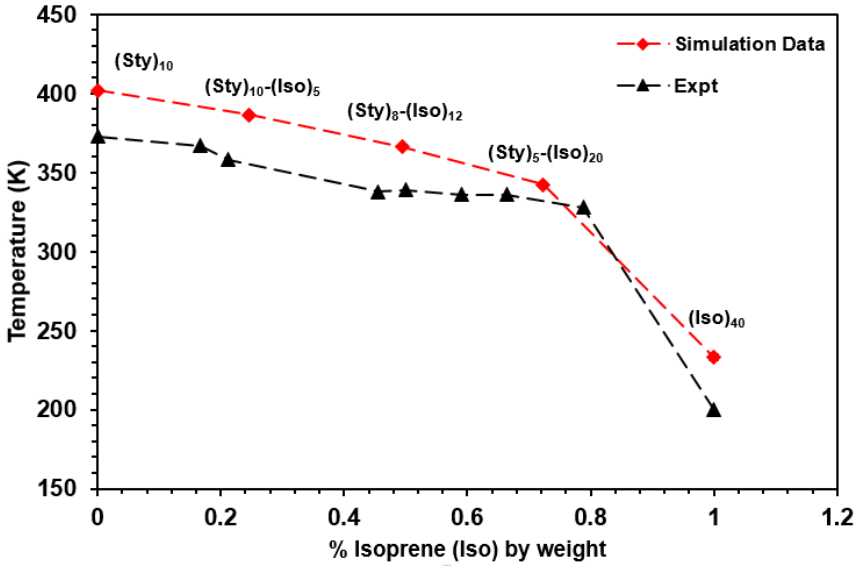

Fig. 4.3: T_g as a function of composition for different Sty-Iso diblock copolymers

4.2 Styrene-Isoprene(H) copolymer:

4.2.1 Densities:

The similar protocol as described in section 3.6 was used for calculations of density dependence on compositions. At 298 K and 1 bar, monomer Isoprene(Iso-H) or Isopentane, has a density of 616 kg/m^3 and simulation gave the density of 630 kg/m^3 which is within the acceptable error of 2.22%.[45] Again the homopolymers of isoprene hydrogenated (IsoH) were constructed with different chain lengths and the densities were calculated. It is observed from the plot 4.4 that the plot plateau's at $(\mathrm{Iso})_{40}$. The IsoH polymer simulations gave a density of 860.76 kg/m^3 which is in a good agreement with the value of 856 kg/m^3 found in the experimental study done by Gotro and Graessley[46]

Styrene (Sty)-Isoprene (Iso) copolymer forcefield

copolymer	Iso (%)	Density (kg/m^3)	Density Expt	%Err	T_g	T_g Expt[9]	% Err
$(Sty)_{10}$	0	1052.56	1052[43]	0.05	401.79	373	7.71
$(Sty)_{10}$-$(Iso)_5$	24.64	1016.47			386.31		
$(Sty)_8$-$(Iso)_{12}$	49.52	978.31			366.28		
$(Sty)_5$-$(Iso)_{20}$	72.35	949.14			342.14		
$(Iso)_{40}$	100	905.32	910[44]	-0.51	233.19	200	16.59

Tab. 4.1: Simulation results for Styrene-Isoprene (Sty-Iso) forcefield

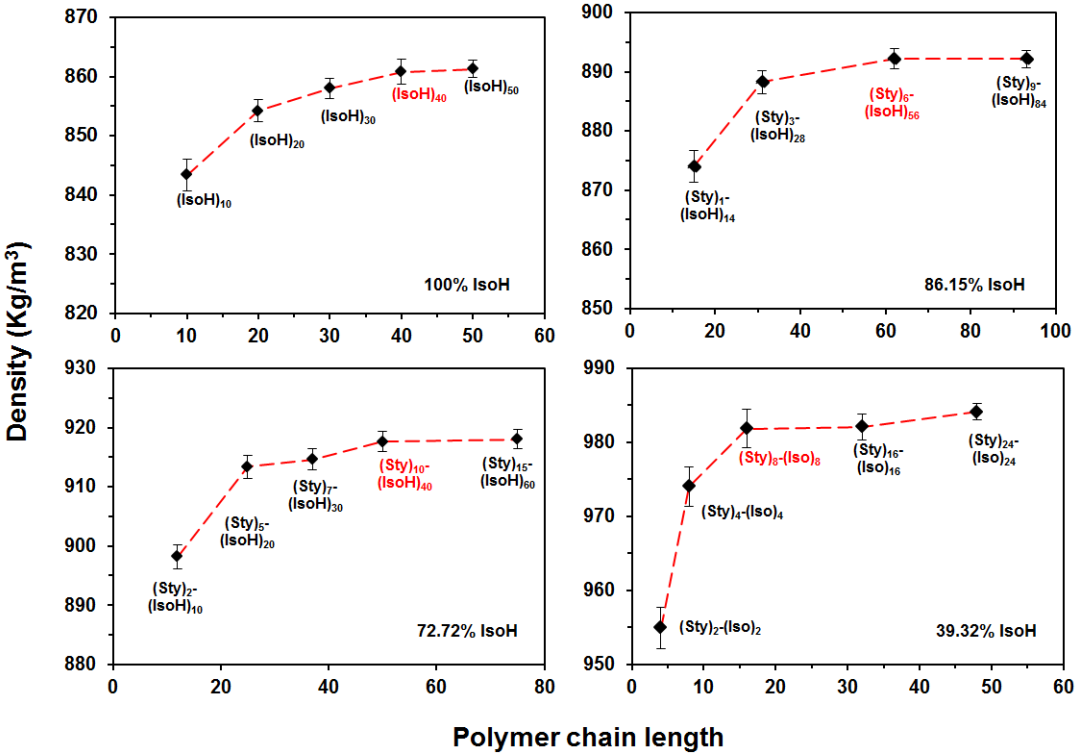

Fig. 4.4: Chain length required for density convergence for different compositions of Sty-IsoH copolymers. Red copolymer is used for further calculations

with a relative error of 0.55%.

Homopolymer forcefields gave good densities compared to the experimental data hence were used for Sty-IsoH copolymers with different compositions. For each composition of copolymer, different chains with varying number of monomers were constructed. Let's say if we want a copolymer with 39.32% IsoH content by weight then different chains such as $(Sty)_2 - (IsoH)_2, (Sty)_4 - (IsoH)_4, (Sty)_8 - (IsoH)_8, (Sty)_{16} - (IsoH)_{16}$ and $(Sty)_{24} - (IsoH)_{24}$ were constructed. All have the same 39.32% IsoH content. Styrene was modeled using the same forcefield from previous studies and was used for copolymers of Sty and IsoH. Same protocol as described in the section 3.6 was used for calculating the chain length dependence on compositions. Plot 4.4 shows that each composition has different chain length at which the density converges. The figure 4.4 shows the chain length dependence on the composition. The copolymer label with red color was used in the further studies.

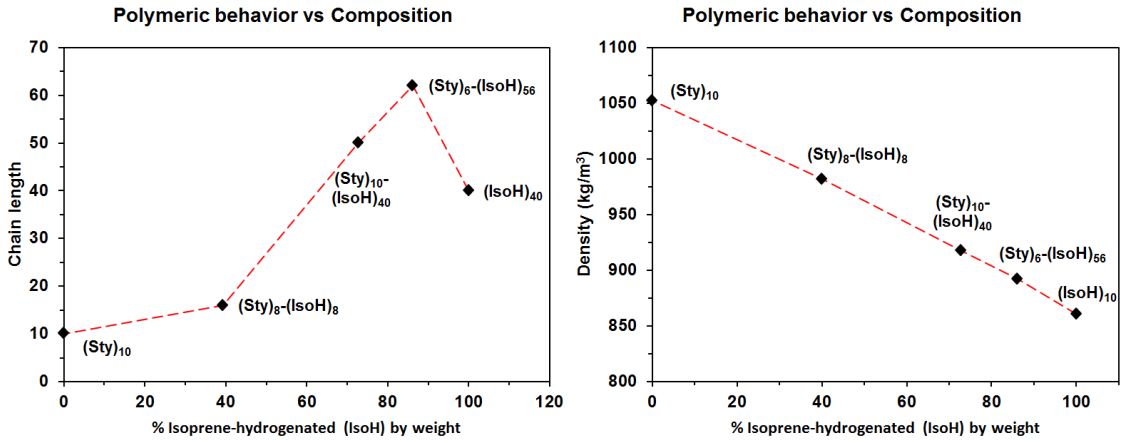

Fig. 4.5: Left: (a) Chain length dependence for polymeric behavior Right: (b) Copolymer densities as a function of composition of Sty-IsoH copolymers

The figure 4.5 shows the minimum chain length required for the polymeric behaviour of the Sty-Iso copolymers. The density as a function of composition follows a linear trend which is again a characteristic of the block copolymers.

4.2.2 Glass transition temperature (T_g):

Similar protocol as described in section 3.7 was used for glass transition temperature calculation. T_g was calculated for homopolymer of Iso-H. The value 224.52 K is in good agreement with the experimental value[39] of 213.5 K with a relative error of 5.16%. The T_g vs composition of the copolymer follows a trend which is similar Sty-Iso copolymer and its is expected to follow similar trend as we have only hydrogenated the isoprene. Unfortunately, due to the unavailability of the experimental data the trend was fitted with equation 3.2 with (k_{KW}=5.68, $q = -93.61$K).

The Sty-IsoH forcefield results (density and glass transition temperature) are summarized in the table 4.1.

Styrene-Isoprene(H) (Sty-IsoH) copolymer forcefield

Polymer	Iso (%)	Density (kg/m^3)	Density Expt	%Err	T_g	T_g Expt	% Err
$(Sty)_{10}$	0	1052.56	1050[43]	0.24	401.79	373[9]	7.5
$(Sty)_{10}$-$(Iso)_5$	39.32	982.08			372.82		
$(Sty)_8$-$(Iso)_{12}$	72.72	917.63			328.97		
$(Sty)_5$-$(Iso)_{20}$	86.15	892.16			295.68		
$(Iso)_{40}$	100	860.76	856[46]	0.55	224.52	213.5[47]	5.16

Tab. 4.2: Simulation results for Styrene-Isoprene (Sty-IsoH) hydrogenated forcefield

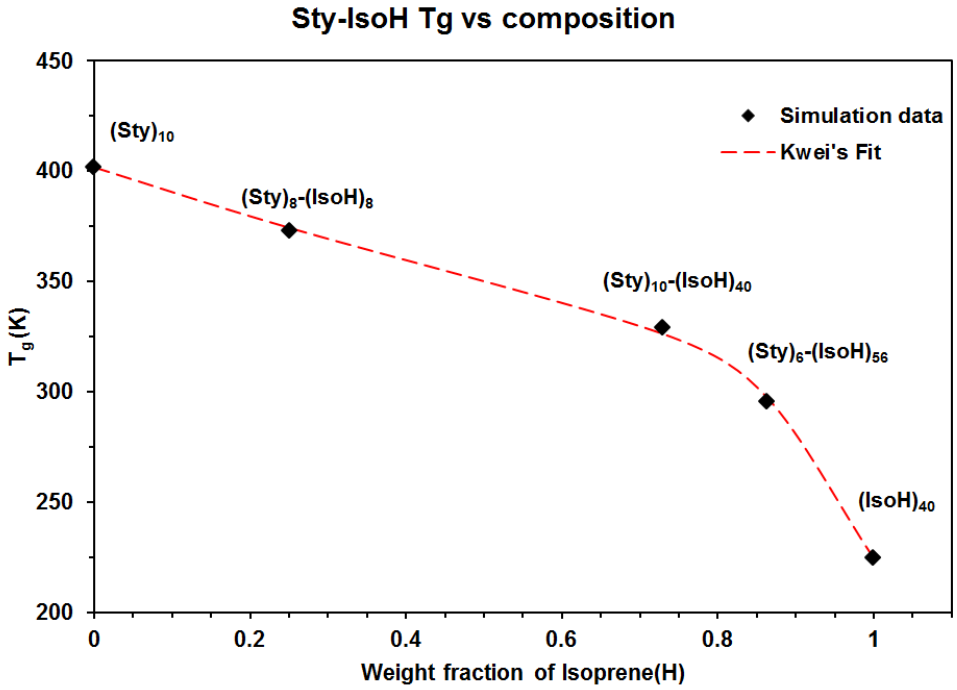

Fig. 4.6: Dependence of T_g on the composition of diblock Sty-IsoH copolymer

4.3 Viscosity Modification

In the coming sections, we study the viscosity modification using the copolymer model that we have developed in the previous studies. We have only considered Sty-IsoH copolymers for the viscosity calculations as they are primarily used as a Viscosity Index Modifier (VIM) in the fuels. The effect of copolymers on the viscosity as a function of temperature as well as composition of base oil (n-hexadecane and n-decylbenzene) was studied. A comparative study of the effect of topology of the copolymer on the viscosity was also done.

4.4 n-hexadecane and n-decylebenzene

n-hexadecane (hex) and n-decylbenzene (dec) were selected as a candidate for the base oil as they serve as surrogates for diesel. In this study, we have studied molecular dynamics simulations of n-decylbenzene and n-hexadecane using three different force fields. The simulations were carried out at both at ambient as well as at high temperature-pressure conditions, to replicate the actual conditions in a diesel injection system. We have compared our simulation results with experimental values of shear viscosity in each case.

The base oil (hex and dec) was modeled using a united atom (UA) and two all atomistic models (AA) (fig. 4.7). In the UA model, CH_3 and CH_2 groups are represented as two different interaction sites in which hydrogen atoms are assumed to be present but implicitly. Specifically, we have used TraPPE[48] united atom model. The second forcefield was an OPLS-AA[17] model. The modified version of the OPLS-AA forcefield optimized for long chain hydrocarbons, also known as LOPLS-AA[49] forcefield was also

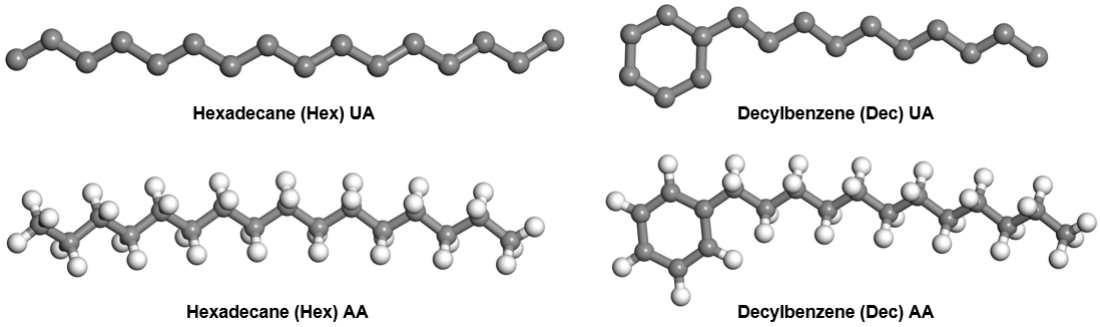

Fig. 4.7: Different types of models used for Hexadecane and Decylbenzene

used. A comparative study of the density and viscosity at different pressures was done in order to select the forcefield appropriate for viscosity calculations with copolymers.

4.4.1 Densities

A similar protocol as discussed in the section 4.1.1 was used for the density calculation for both n-dec and n-hex as a function of pressure. We have simulated the system till the pressure 2000 bar at a constant temperature of 423K. The results are showed in the fig. 4.8. We can see that for hexadecane, UA model over predicts the density with all the densities within the acceptable error of 2%. Both AA atom models under predicts the densities. In the case of AA models, OPLS-AA does a better at lower pressures. At the higher pressure of 2000 bar both the AA forcefields have deviated by 3.77% and 3.28% for OPLS-AA and LOPLS-AA respectively. Hence, the UA model is favored over AA models due to better densities at different pressure conditions.

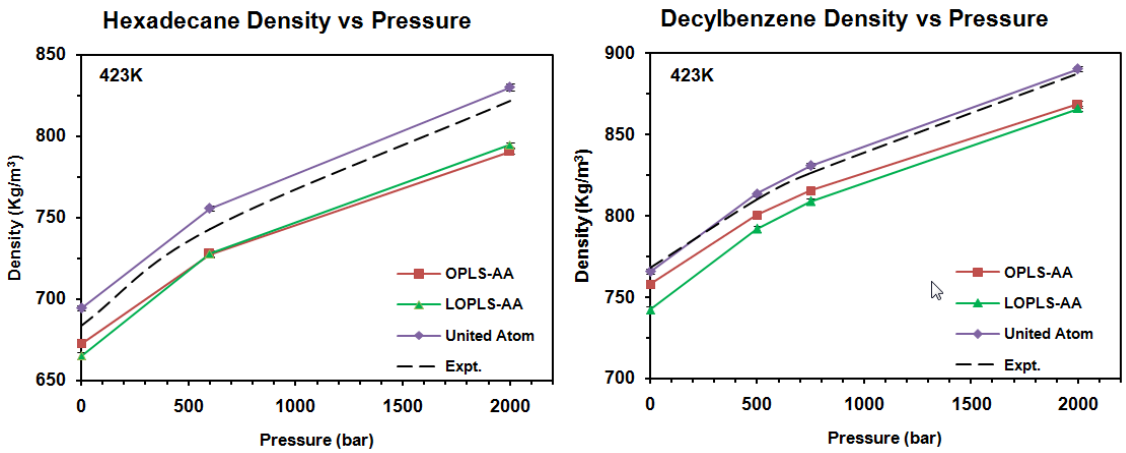

Fig. 4.8: Density dependence on pressure for n-hexadecane (left) and n-decylbenzene (right) for different models at 423K.

In the case of n-decylbenzene, UA model again over predicts the densities with a deviation of within 1% from the experimental values. In the case of AA models, both of them under-predicts the densities. OPLS-AA does a better job at the lower pressure of 1bar with an error of 1.35% while LOPLS-AA giving an error of 3.37% from the experimental value of 768 kg/m^3. At high pressures of 500, 750 and 2000 bar both AA

forcefields behaves similarly. The error was 2.11% and 2.41% from the experimental value of 887.4 kg/m^3 at 2000 bar for OPLS-AA and LOPLS-AA respectively. The results show that UA model is better at producing densities for n-decylbenzene as well as n-hexadecane at different pressure conditions with a constant temperature of 423K. The results are summarized in the table 4.3.

n-decylbenzene and n-hexadecane density

Molecule	Pressure	ρ (expt)[50] (kg/m^3)	OPLS-AA	LOPLS-AA	TraPPE-UA
n-dec	1 bar	768.3	757.91	742.40	765.97
n-dec	500 bar	810	800.40	792.03	813.68
n-dec	750 bar	826.4	815.41	808.95	830.98
n-dec	2000 bar	887.4	868.67	866.0	890.26
n-hex	1 bar	683.3	672.55	665.0	694.41
n-hex	600 bar	743.2	727.42	727.73	755.67
n-hex	2000 bar	821.7	790.71	794.68	830.0

Tab. 4.3: Density results for n-hexadecane and n-decylbenzene at 423 K

4.4.2 Viscosity of Decylbenzene and Hexadecane

The forcefields were used for calculating the viscosities using Green-Kubo method (2.3) as described in section 3.8 at 423K with varying pressures. They were compared with experimental data. The plot 4.9 shows the viscosity of n-hexadecane calculated from 10 independent trajectories at different pressure conditions. It can be seen that, all the three models do fairly well at the lower pressure of 1 bar while under-predicting the viscosities at higher pressures. UA model performs badly at high pressures of 2000 bar with an error of 75%.[50] Within the two AA models, better performance was expected from the LOPLS-AA model as the parameters are optimized for long chain hydrocarbons but the opposite was observed from the viscosity studies.

A similar behaviour was observed for n-decylbenzene. It can be seen from the plot 4.10 that both the AA models are giving good results at ambient pressure conditions (423K) with a deviation of 3.37% (LOPLS-AA), 4.4% (OPLS-AA) and 10.45% (TraPPE-UA) from the experimental value of 0.61 mP.[50] UA model again under-predicts the viscosities compared to both the AA models at higher pressures. In the case of AA models, OPLS-AA gives marginally better results at higher pressures.

Comparing the density results for both n-decylbenzene and n-hexadecane, TraPPE-UA does better while performs badly in the viscosity calculations at higher pressures. In the case AA-models, both gives similar density results but OPLS-AA does better in the viscosity calculations at higher pressures. Hence, OPLS-AA model was used for the viscosity calculations involving copolymers and solvent. The results are summarized in the table 4.4.

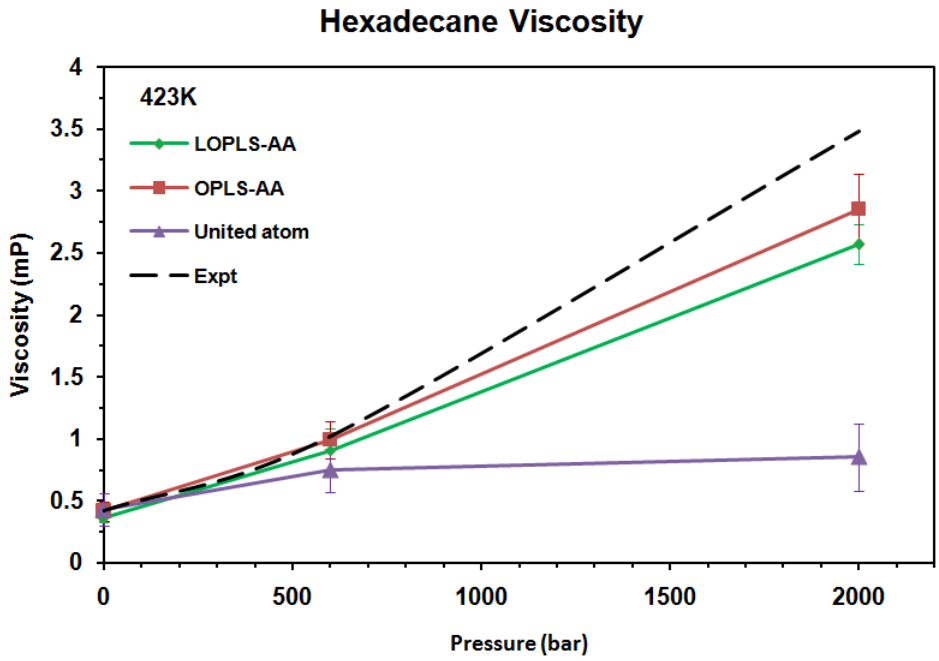

Fig. 4.9: n-hexadecane (hex) viscosity with different forcefields at 423K

n-decylbenzene and n-hexadecane viscosity

Molecule	Pressure	η (expt)[50] (mP)	OPLS-AA	LOPLS-AA	TraPPE-UA
n-dec	1 bar	0.61	0.583	0.610	0.546
n-dec	500 bar	1.3	1.192	1.042	0.874
n-dec	750 bar	1.92	1.545	1.391	0.914
n-hex	1 bar	0.42	0.417	0.366	0.431
n-hex	600 bar	1.02	0.995	0.911	0.746
n-hex	2000 bar	3.49	2.860	2.572	0.854

Tab. 4.4: Viscosity of n-hexadecane and n-decylbenzene at 423K

4.5 Solvent compositions

In an oil, a composition of n-decylbenzene and n-hexadecane is used. Hence, the model should also give good viscosity results for different compositions of n-dec and n-hex. The OPLS-AA was used for the viscosity calculations for the solvent composition as it gave good results for individual density as well as viscosity calculations. Different compositions in ratio such as 0.2:0.8, 0.4:0.6, 0.6:0.4 and 0.8:0.2 (n-decylbenzene:n-hexadecane) were made. The total number of molecules in all the compositions were 200.

Similar protocol as described in the section 3.8 was used for these calculations. Viscosity calculation was performed at 423K and 1 bar. The plot 4.11 shows that the OPLS-AA forcefield is able to reproduce the experimental data.[50] The same forcefield was used for solvent plus copolymer viscosity calculations. The results are summarized in the table 4.5

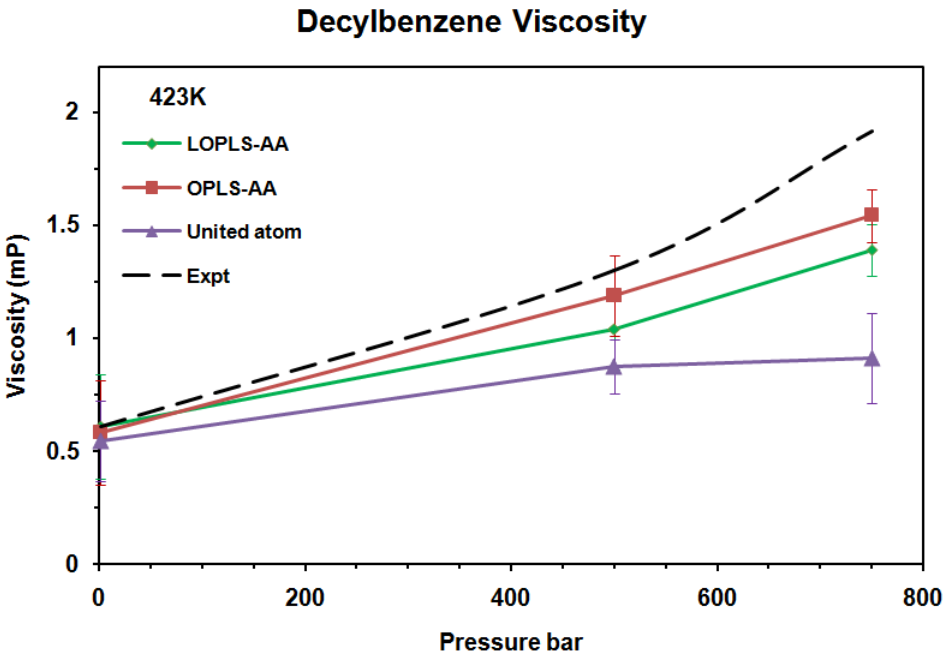

Fig. 4.10: Viscosity of n-decylbenzene with different forcefields at 423 K

n-decylbenzene and n-hexadecane binary mixture viscosity

n-dec (mols)	n-hex (mols)	η (expt)[50] (mP)	Sim. (η) (OPLS-AA)	% err
200	0	0.61	0.592	-2.95
3200	800	0.57	0.584	2.45
2400	1600	0.59	0.587	-0.50
1600	2400	0.57	0.564	-1.05
800	3200	0.57	0.560	-1.75
0	200	0.42	0.417	0.71

Tab. 4.5: Viscosity results for n-hexadecane and n-decylbenzene mixtures at 423 K

4.6 Co-polymer and base oil

The copolymers Sty-Iso and Sty-IsoH are used as Viscosity Index Modifiers (VIM's), hence, the important property that needs to be investigated is Viscosity modification by these copolymers. In these studies, we have particularly considered the copolymers of Sty-IsoH as they are being used preferentially over the copolymers of Sty-Iso because of the better VI modifying properties. The effect of different topologies such as block and the tapered copolymer was studied. The figure 4.12 shows the block and tapered copolymer used in this study. A single chain of both of them contains exactly the same number of Styrene and Isoprene(H) monomers.

4.6.1 Effect of topology

The effect of adding 10 copolymers in the different compositions of the n-hexadecane and n-decylbenzene at 423 K and 1 bar was studied. $(\text{Sty})_{21} - (\text{IsoH})_{21}$ and Tapered_{42} was used for the study. From the fig. 4.13 it can be seen that with the addition of

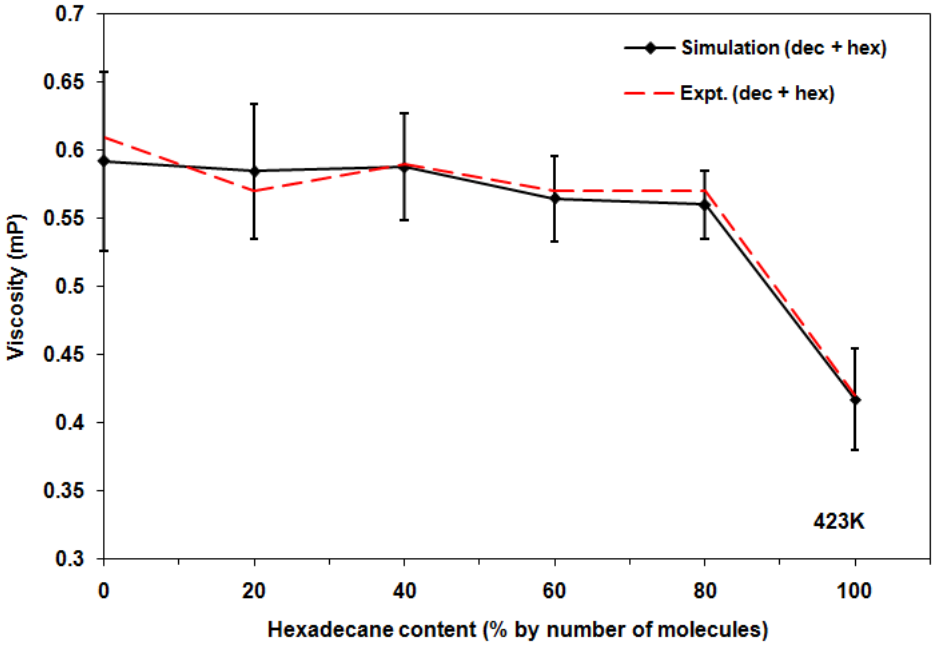

Fig. 4.11: Solvent (n-dec + n-hex) viscosity with different compositions at 423K

copolymers there is indeed enhancement in the viscosity when compared with pure base oil. The block copolymer gives higher viscosity enhancement compared tapered copolymer.

At 80% hexadecane content, the increase in the viscosity is minimal while at 20% it is relatively high. This shows that viscosity modification is mostly dependent on the n-decylbenzene content as the number of styrene monomers in each (block and tapered) copolymers are same. We believe the stacking interactions between styrenes of the copolymer and n-decylbenzene are responsible for the higher viscosity enhancement in the compositions of solvent with higher percentage of the n-decylbenzene.

4.6.2 Effect of temperature

We have studied the effect of temperature on the viscosity of the four systems containing 2000:2000 molecules mixture of n-dec and n-hex with 10 and 5 copolymers of $(\mathrm{Sty})_{21} - (\mathrm{IsoH})_{21}$ and $\mathrm{Tapered}_{42}$ each. The viscosity was calculated using the protocol described in the section 3.8. The calculation was done at three temperatures being 373 K, 423 K and 473K at 1 bar pressure.

The plot 4.14 shows the effect of number and topology of copolymers on viscosity with respect to the temperature. We can see that viscosity is dependent upon the concentration of the copolymers. Block copolymer has higher viscosity enhancement with 10 block copolymers (blue) compared to 5 block copolymers (red). Similar results are observed with tapered copolymers showing higher viscosity with 10 tapered copolymers (green) compared to five (black). A good viscosity index modifier (VIM) should improve the Viscosity Index (VI) of the fluid, meaning the viscosity dependence with temperature should be small. Even though the viscosity modification is higher in the case of block copolymers the slope of the viscosity vs temperature plot is lower for ta-

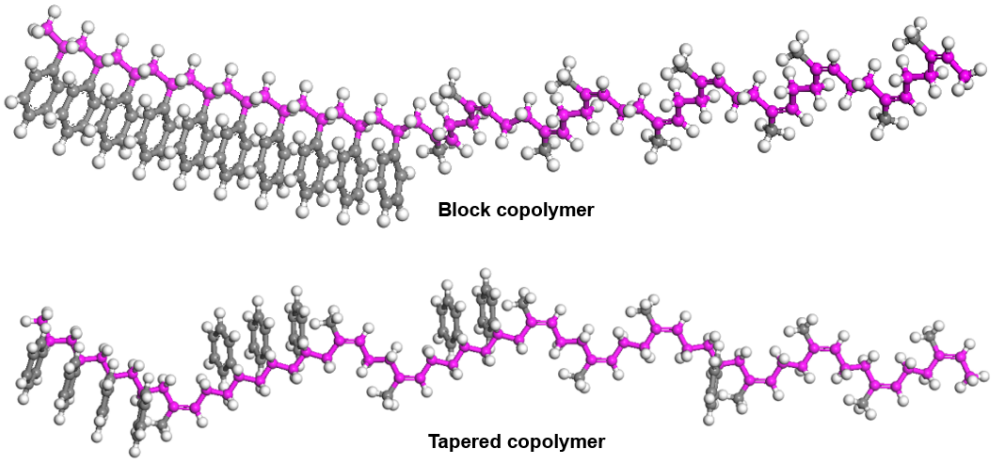

Fig. 4.12: Block and tapered copolymer models

pered copolymer with both ten and five copolymers. Hence the viscosity-temperature dependence is lower for the tapered copolymers. Therefore we can conclude that the tapered copolymers is a better Viscosity Index Modifier (VIM).

The radius of gyration (R_g) (section: A.1) gives the idea about the size of the molecule. The R_g for each of the copolymer (block and tapered) was calculated from 10 independent trajectories. From the plot 4.15a it can be seen that block copolymer has higher R_g at all the temperature conditions compared to the tapered copolymer. Same was observed from the end-to-end (ete) distance plot 4.15b which gives information about the distance between one end of the copolymer from the other. Both the R_g and the ete are higher in the case of block copolymer suggesting larger size of the copolymer leading to higher interactions with solvent, hence the higher viscosity enhancement.

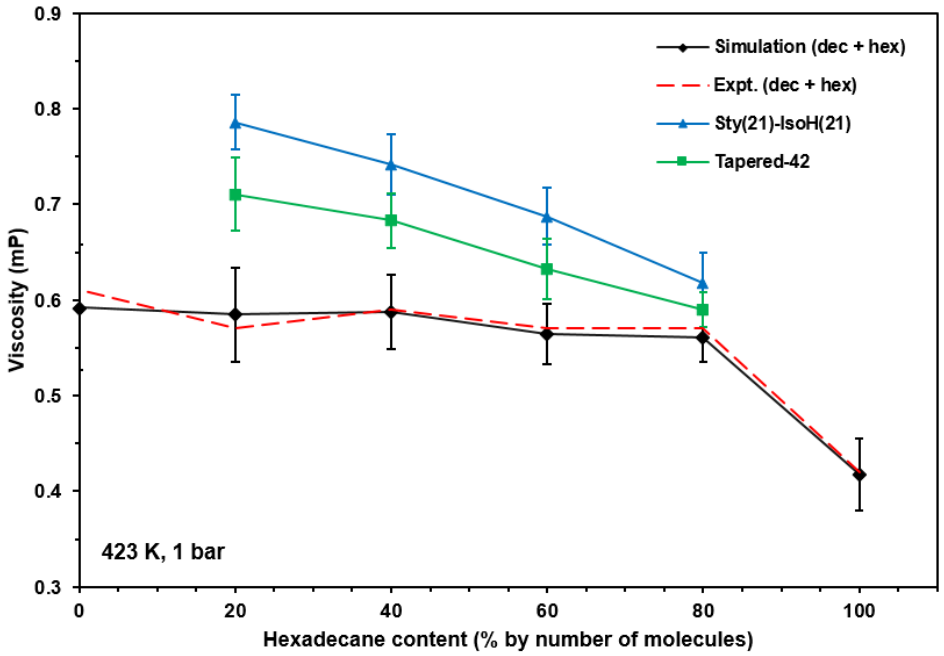

Fig. 4.13: Viscosity of different compositions of solvent with and without block and tapered copolymer at 423 K and 1 bar

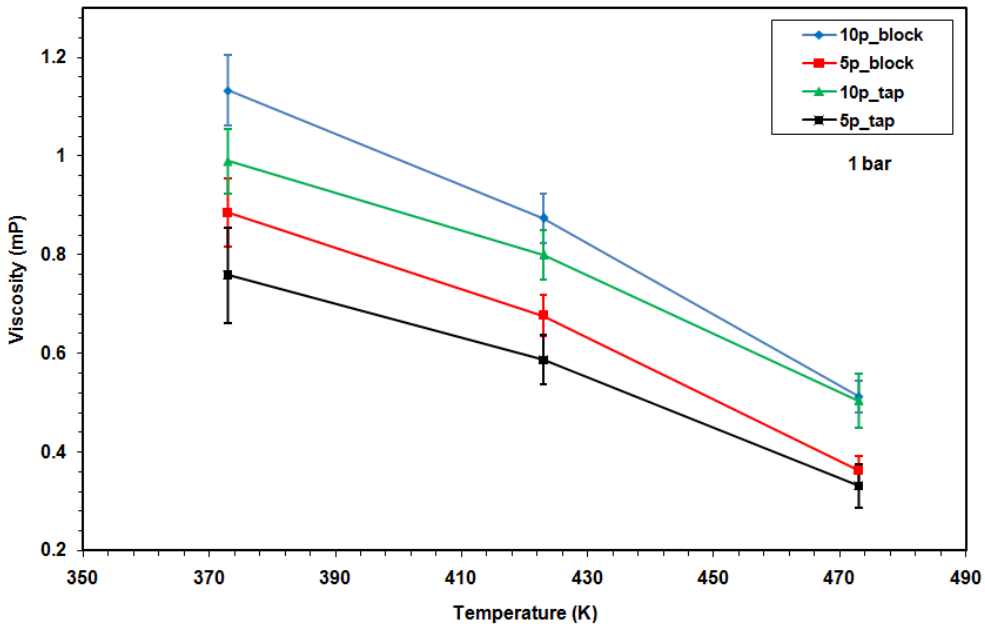

Fig. 4.14: Effect topology and number of copolymers with varying temperatures and a constant pressure of 1 bar

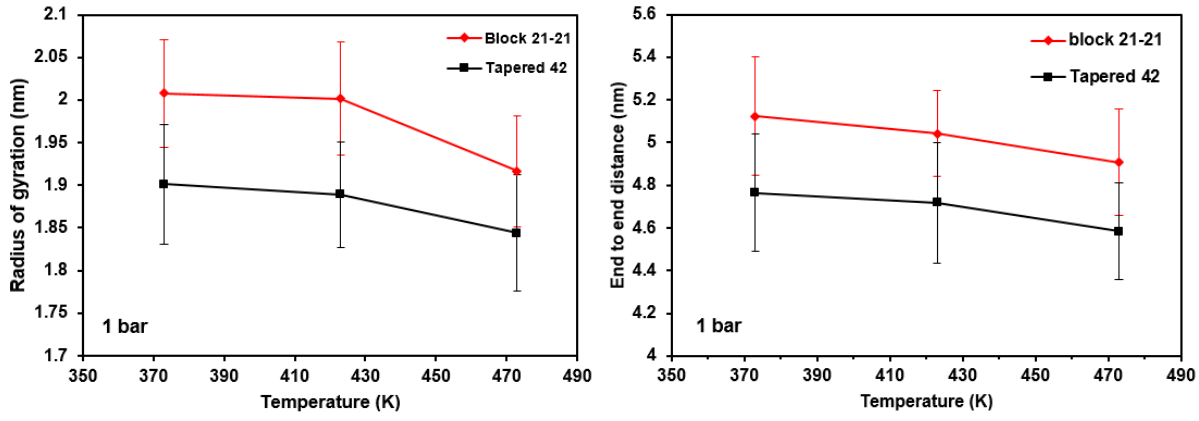

(a) (b)

Fig. 4.15: (a) Effect of temperature on the radius of gyration (R_g) (b) end to end distance (ete) for $(Sty)_{21} - (IsoH)_{21}$ and $Tapered_{42}$ at 1 bar

5. CONCLUSIONS

Copolymers are interesting kind of macro-molecules which give similar properties of the constituent homopolymers and have found many applications including as additives in the fuels. With two extra dihedrals and partial charges, we have developed an all-atomistic forcefield for Styrene-Isoprene copolymers. Using 16 different types of residues, we have made a framework for constructing different types of topologies including block and tapered copolymers.

It was observed that each copolymer has a chain length dependence on density which plateau's after a particular chain length. This chain length should be minimum one should use in an MD simulation. The similar study was repeated for different compositions of the copolymer. The polyisoprene and polystyrene densities were in very good agreement with experimental values. The densities of the copolymer with different compositions shows a nice linear relationship, which is characteristic of copolymers. Glass transitions temperatures of the Sty-Iso copolymers were also in good agreement with experimental values with a similar trend.

In the case of Styrene-Isoprene hydrogenated copolymer, a similar study was done in order to find minimum chain length for polymeric behaviour. The homopolymer densities were in good agreement with experiments within 1% error. The density as a function of the composition of copolymers follows a linear trend. T_g's obtained for homopolymers were in good agreement with an error of 4.42% for polyisoprene hydrogenated and 4.5% for polystyrene. The trend was similar to the Sty-Iso copolymer results. Again the T_g as a function of composition was fitted with Kwei's relation. Having obtained the densities and T_g's, the viscosity modifying properties of the Sty-IsoH copolymer studied using Green-Kubo method.

Diesel surrogates n-hexadecane and n-decylbenzene were used as base fuel. Different forcefields such as LOPLS-AA, OPLS-AA and TraPPE-UA were used. OPLS-AA did better in viscosity properties of the base oil than UA model and marginally better than LOPLS-AA forcefield. Hence, the OPLS-AA was used for the viscosity calculations. The addition of copolymers to the base oil indeed increases the viscosity of the fluid mixture which is also dependent on the copolymer concentration. The viscosity enhancement was observed to be higher with the higher content of n-decylbenzene in the mixture, which suggests that the benzene stacking interactions are important in viscosity modification for these copolymers. The viscosity enhancement in the case of block copolymers was higher compared to a tapered copolymer with exactly the same number of styrenes and isoprenes(H) in a chain. The R_g and the end-to-end distance results suggest that the block copolymer is bigger in size compared to the tapered copolymer, resulting in a higher number of interactions with the fuel and hence the viscosity enhancement.

In conclusion, equilibrium molecular dynamics (MD) simulations can be used to calculate the viscosity of the complex fluid such as copolymer and fuel. One needs to span the whole phase space in order to get approximately correct viscosity estimation. Using Green-Kubo method one can get viscosity estimation of the solvent within the relative error of 5% from the experimental values for the all-atom as well as united atom forcefields at ambient pressure and high temperature conditions of 423 K. But the viscosity prediction at higher pressures is still a challenge. Our viscosity simulations were limited to the pressure of 1 bar as all the forcefields we tried could not reproduce the experimental viscosity at high pressures after 750 bar, united atom model being highly erroneous of all. This could be achieved by fine tuning the forcefields or implementing other viscosity prediction methods such as Transverse Current Autocorrelation function (TCAF).

In future, the atomistic model of the copolymers will be used to develop course grained models, in which one represents a group of atoms as a one bead. This drastically reduces the computational cost and allows us to reach higher lengthscales as well as timescales. This could be used to screen several VIMs with different topologies and chemistries to identify high performance materials.

Appendices

Appendix A

A.1 Radius of gyration (R_g)

Radius of gyration gives the idea about dimensions of the polymer chains and is given by

$$R_g = \left(\frac{\sum_i \|r_i\|^2 m_i}{\sum_i m_i} \right)^{\frac{1}{2}} \tag{A.1}$$

where m_i is the mass of atom i and r_i the positions of atom i with respect to the center of mass of the molecule.

A.2 End to end distance

End to end distance is the distance between the polymers starting residue and the last residue. It helps us to understand if the polymer is in globule state or the extended state.

A.3 Forcefield parameters:

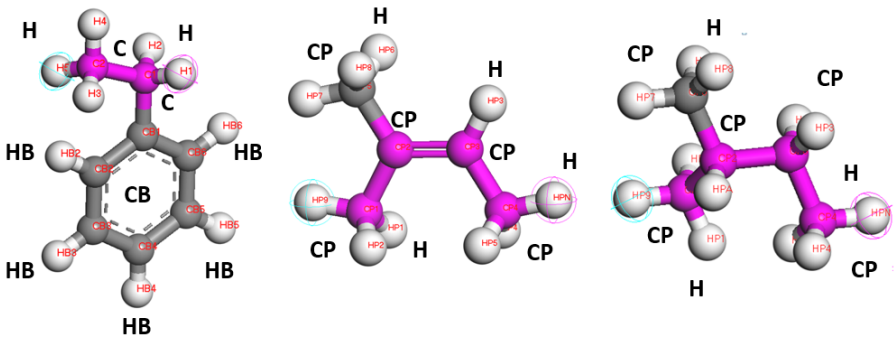

Fig. A.1: Sty, Iso and IsoH models

Molecule	Atomtypes	σ (nm)	ϵ (kj/mol)
Isoprene	CP	0.35	0.276144
	HP	0.25	0.12552
Styrene	C	0.3207	0.294
	CB	0.355	0.294
	H	0.2318	0.318
	HB	0.242	0.126
Isoprene(H)	CP	0.35	0.276144
	HP	0.25	0.12552

Tab. A.1: Lennard-Jones parameters

Molecule	Bonds	r_0 (nm)	K_b (kj/mol)
Sty-Iso	CP-C	0.1529	224262.4
Sty-IsoH	CP-C	0.1529	224262.4
Isoprene	CP-CP	0.1529	224262.4
	CP-HP	0.109	284512
Styrene	CB-H	0.108	200000
	C-CB	0.151	265646
	C-C	0.153	259780

Tab. A.2: Bond parameters

Molecule	Angles	θ_0	K_0 (kj/mol)
Isoprene	CP-CP-CP	112.7	488.273
	CP-CP-H	110.7	313.8
	H-CP-H	107.8	276.144
Styrene	CB-CB-CB	120	376.6
	CB-CB-C	120	376.6
	CB-CB-H	120	418.8
	C-C-C	109.45	366.9
	C-C-H	109.45	366.9
	H-C-H	109.45	306.4
Sty-Iso	CP-C-C	109.45	366.9
	CP-C-CB	109.45	482.3
	C-CP-CP	109.45	250
Sty-IsoH	CP-C-C	109.45	366.9
	CP-C-CB	109.45	482.3
	C-CP-CP	109.45	250

Tab. A.3: Angle parameters

Molecule	Dihedral	Type	Parameters (kj/mol)
Isoprene	CP-CP-CP-CP	Ryckaert-Bellemans	2.929, -1.464, 0.209, -1.6736, 0, 0
	CP-CP-CP-HP	Ryckaert-Bellemans	0.6276, 1.8828, 0, -2.5104, 0, 0
Styrene	C-C-C-C	Fourier dihedral	0, 0, 12, 0
	C-C-CB-CB	Fourier dihedral	0.3782, -4.5713, 0.3254, 0
Sty-Iso	CB-C-CP-CP	Ryckaert-Bellemans	2.929, -1.464, 0.209, -1.6736, 0, 0
	C-C-CP-CP	Ryckaert-Bellemans	2.929, -1.464, 0.209, -1.6736, 0, 0
Sty-IsoH	CB-C-CP-CP	Ryckaert-Bellemans	2.929, -1.464, 0.209, -1.6736, 0, 0
	C-C-CP-CP	Fourier dihedral	0, 0, 12, 0

Tab. A.4: Dihedral parameters

BIBLIOGRAPHY

[1] TW Selby. The non-newtonian characteristics of lubricating oils. *ASLE Transactions*, 1(1):68–81, 1958.

[2] VA Harmandaris, M Doxastakis, VG Mavrantzas, and DN Theodorou. Detailed molecular dynamics simulation of the self-diffusion of n-alkane and cis-1, 4 polyisoprene oligomer melts. *The Journal of chemical physics*, 116(1):436–446, 2002.

[3] Michael J Covitch, Kieran J Trickett, et al. How polymers behave as viscosity index improvers in lubricating oils. *Advances in Chemical Engineering and Science*, 5(02):134, 2015.

[4] Standard practice for calculating viscosity index from kinematic viscosity at 40 and 100˚c. *ASTM, D2270*, aug.

[5] Thomas Q Chastek. Improving cold flow properties of canola-based biodiesel. *biomass and bioenergy*, 35(1):600–607, 2011.

[6] Abdel-Azim A Abdel-Azim and Rash M Abdel-Aziem. Polymeric additives for improving the flow properties and viscosity index of lubricating oils. *Journal of Polymer Research*, 8(2):111–118, 2001.

[7] M Mondello, Hyung-Jin Yang, Hidemine Furuya, and Ryong-Joon Roe. Molecular dynamics simulation of atactic polystyrene. 1. comparison with x-ray scattering data. *Macromolecules*, 27(13):3566–3574, 1994.

[8] John D Ferry. *Viscoelastic properties of polymers*. John Wiley & Sons, 1980.

[9] Gert R Strobl and Gert R Strobl. *The physics of polymers*, volume 2. Springer, 1997.

[10] Encyclopædia Britannica. polyisoprene date accessed 19th mar. 2016. http://www.britannica.com/science/polyisoprene.

[11] Norman R Legge. Thermoplastic elastomers. *Rubber Chemistry and Technology*, 60(3):83–117, 1987.

[12] Napida Hinchiranan, Kitikorn Charmondusit, Pattarapan Prasassarakich, and Garry L. Rempel. Hydrogenation of synthetic cis-1,4-polyisoprene and natural rubber catalyzed by [ir(cod)py(pcy3)]pf6. *Journal of Applied Polymer Science*, 100(5):4219–4233, 2006.

[13] Chang Dae Han, Deog Man Baek, Jin Kon Kim, Toshihiro Ogawa, Naoki Sakamoto, and Takeji Hashimoto. Effect of volume fraction on the order-disorder transition in low molecular weight polystyrene-block-polyisoprene copolymers. 1. order-disorder transition temperature determined by rheological measurements. *Macromolecules*, 28(14):5043–5062, 1995.

[14] NR Legge. Thermoplastic elastomers-three decades of progress. *Rubber chemistry and technology*, 62(3):529–547, 1989.

[15] Andrew R. Leach. *Molecular Modelling: Principles and Applications*. Prentice Hall, 2001.

[16] Sir john a. pople, 1925-2004. *Journal of computational chemistry*, 25(9), jul 2004.

[17] William L Jorgensen, David S Maxwell, and Julian Tirado-Rives. Development and testing of the opls all-atom force field on conformational energetics and properties of organic liquids. *Journal of the American Chemical Society*, 118(45):11225–11236, 1996.

[18] Lars Onsager. Electric moments of molecules in liquids. *Journal of the American Chemical Society*, 58(8):1486–1493, 1936.

[19] Berk Hess. Determining the shear viscosity of model liquids from molecular dynamics simulations. *The Journal of chemical physics*, 116(1):209–217, 2002.

[20] Bruce J Palmer. Transverse-current autocorrelation-function calculations of the shear viscosity for molecular liquids. *Physical Review E*, 49(1):359, 1994.

[21] Melville S Green. Markoff random processes and the statistical mechanics of time-dependent phenomena. ii. irreversible processes in fluids. *The Journal of Chemical Physics*, 22(3):398–413, 1954.

[22] Ryogo Kubo. Statistical-mechanical theory of irreversible processes. i. general theory and simple applications to magnetic and conduction problems. *Journal of the Physical Society of Japan*, 12(6):570–586, 1957.

[23] Robert Zwanzig. Time-correlation functions and transport coefficients in statistical mechanics. *Annual Review of Physical Chemistry*, 16(1):67–102, 1965.

[24] Roland Faller, Florian Müller-Plathe, Manolis Doxastakis, and Doros Theodorou. Local structure and dynamics of trans-polyisoprene oligomers. *Macromolecules*, 34(5):1436–1448, 2001.

[25] Pragati Sharma, Sudip Roy, and Hossein Ali Karimi-Varzaneh. Validation of force fields of rubber through glass transition temperature calculation by microsecond atomic-scale molecular dynamics simulation. *The Journal of Physical Chemistry B*, 2016.

[26] Roland Faller and Dirk Reith. Properties of poly (isoprene): model building in the melt and in solution. *Macromolecules*, 36(14):5406–5414, 2003.

[27] M Doxastakis, DN Theodorou, G Fytas, F Kremer, R Faller, Florian Müller-Plathe, and N Hadjichristidis. Chain and local dynamics of polyisoprene as probed by experiments and computer simulations. *The Journal of chemical physics*, 119(13):6883–6894, 2003.

[28] Collin D Wick, Marcus G Martin, and J Ilja Siepmann. Transferable potentials for phase equilibria. 4. united-atom description of linear and branched alkenes and alkylbenzenes. *The Journal of Physical Chemistry B*, 104(33):8008–8016, 2000.

[29] Marco Fioroni and Dieter Vogt. Toluene model for molecular dynamics simulations in the ranges 298< t (k)< 350 and 0.1< p (mpa)< 10. *The Journal of Physical Chemistry B*, 108(31):11774–11781, 2004.

[30] Jie Han, Richard H Gee, and Richard H Boyd. Glass transition temperatures of polymers from molecular dynamics simulations. *Macromolecules*, 27(26):7781–7784, 1994.

[31] Roland F Rapold, Ulrich W Suter, and Doros N Theodorou. Static atomistic modelling of the structure and ring dynamics of bulk amorphous polystyrene. *Macromolecular theory and simulations*, 3(1):19–43, 1994.

[32] Hu-Jun Qian, Paola Carbone, Xiaoyu Chen, Hossein Ali Karimi-Varzaneh, Chee Chin Liew, and Florian Müller-Plathe. Temperature-transferable coarse-grained potentials for ethylbenzene, polystyrene, and their mixtures. *Macromolecules*, 41(24):9919–9929, 2008.

[33] Curt M Breneman and Kenneth B Wiberg. Determining atom-centered monopoles from molecular electrostatic potentials. the need for high sampling density in formamide conformational analysis. *Journal of Computational Chemistry*, 11(3):361–373, 1990.

[34] Berk Hess, Carsten Kutzner, David Van Der Spoel, and Erik Lindahl. Gromacs 4: algorithms for highly efficient, load-balanced, and scalable molecular simulation. *Journal of chemical theory and computation*, 4(3):435–447, 2008.

[35] Herman JC Berendsen, JPM van Postma, Wilfred F van Gunsteren, ARHJ DiNola, and JR Haak. Molecular dynamics with coupling to an external bath. *The Journal of chemical physics*, 81(8):3684–3690, 1984.

[36] Berk Hess. P-lincs: A parallel linear constraint solver for molecular simulation. *Journal of Chemical Theory and Computation*, 4(1):116–122, 2008.

[37] PG Santangelo and CM Roland. Molecular weight dependence of fragility in polystyrene. *Macromolecules*, 31(14):4581–4585, 1998.

[38] Xinya Lu and Bingzheng Jiang. Glass transition temperature and molecular parameters of polymer. *Polymer*, 32(3):471–478, 1991.

[39] N Hinchiranan, P Prasassarakich, and GL Rempel. Hydrogenation of natural rubber in the presence of oshcl (co)(o2)(pcy3) 2: Kinetics and mechanism. *Journal of applied polymer science*, 100(6):4499–4514, 2006.

[40] TK Kwei. The effect of hydrogen bonding on the glass transition temperatures of polymer mixtures. *Journal of Polymer Science: Polymer Letters Edition*, 22(6):307–313, 1984.

[41] Zofia Funke, Yohei Hotani, Toshiaki Ougizawa, Jörg Kressler, and Hans-Werner Kammer. Equation-of-state properties and surface tension of ethylene–vinyl alcohol random copolymers. *European polymer journal*, 43(6):2371–2379, 2007.

[42] Cornelius T Moynihan, Allan J Easteal, James Wilder, and Joseph Tucker. Dependence of the glass transition temperature on heating and cooling rate. *The Journal of Physical Chemistry*, 78(26):2673–2677, 1974.

[43] DG Sharp and JW Beard. Size and density of polystyrene particles measured by ultracentrifugation. *Journal of Biological Chemistry*, 185(1):247–253, 1950.

[44] Lewis J Fetters, David J Lohse, and William W Graessley. Chain dimensions and entanglement spacings in dense macromolecular systems. *Journal of Polymer Science Part B: Polymer Physics*, 37(10):1023–1033, 1999.

[45] James Wei. Molecular symmetry, rotational entropy, and elevated melting points. *Industrial & engineering chemistry research*, 38(12):5019–5027, 1999.

[46] JT Gotro and William W Graessley. Model hydrocarbon polymers: rheological properties of linear polyisoprenes and hydrogenated polyisoprenes. *Macromolecules*, 17(12):2767–2775, 1984.

[47] N Hinchiranan, P Prasassarakich, and GL Rempel. Hydrogenation of natural rubber in the presence of oshcl (co)(o2)(pcy3) 2: Kinetics and mechanism. *Journal of applied polymer science*, 100(6):4499–4514, 2006.

[48] Marcus G Martin and J Ilja Siepmann. Transferable potentials for phase equilibria. 1. united-atom description of n-alkanes. *The Journal of Physical Chemistry B*, 102(14):2569–2577, 1998.

[49] Shirley WI Siu, Kristyna Pluhackova, and Rainer A Böckmann. Optimization of the opls-aa force field for long hydrocarbons. *Journal of chemical theory and computation*, 8(4):1459–1470, 2012.

[50] D.M. Doyle A. Verma, I. Rudra and R.F. Cracknell. Prediction of density and viscosity of binary mixtures of diesel fuel surrogates under crdi engine operating conditions. *Shell internal report*.